Short Communication

On the Preparation of Mg$_2$Ni by Combining Electrodeoxidation and Electrolysis Techniques

Fuat ERDEN[1,2,3], İshak KARAKAYA[1] and Metehan ERDOĞAN[4,*]

[1]Metallurgical and Materials Engineering Department, Middle East Technical University, 06800, Ankara, Türkiye
[2]Present Address: Institute of Materials Research and Engineering (IMRE), A*STAR, 3 Research Link, Singapore
[3]Present Address: Materials Science and Engineering Department, National University of Singapore, Singapore
[4]Materials Engineering Department, Yıldırım Beyazıt University, 06220, Ankara, Türkiye
Corresponding author. PhD.
[*]E-mail: metehanerdogan@ybu.edu.tr

Mg$_2$Ni is a well-known hydrogen storage alloy. Most of the preparative methods for this alloy require high temperature processing of pure magnesium and nickel. The proposed method, studied in this work, involves the production of Mg$_2$Ni alloy directly from NiO and MgCl$_2$ in an electrochemical cell. This method can eliminate the difficulties that may arise, during handling due to the reactive nature of metallic components, especially Mg. XRD patterns of reduced samples indicated the partial formation of Mg$_2$Ni. Experimental results also showed that sintering of NiO, which resulted in the decrease of porosities, adversely affects the formation of Mg-Ni intermetallic compounds. Such an observation was thought to be the result of higher molar volume of Mg$_2$Ni as compared to that of NiO.

1. INTRODUCTION

Fossil fuels are widely used, throughout the world, due to their definite advantages over non-conventional energy sources. However, they are not renewable and their usage cause critical environmental problems. Hydrogen, on the other hand, is known as a clean, renewable energy source and instead of fossil fuels; its use for energy production purposes will clearly be environmentally friendly. However, there exist problems that hinder widespread use of hydrogen for energy production. One of these problems is associated with the large-scale storage of hydrogen [1]. Primarily, hydrogen

can be stored in three different ways, (i) as pressurized gas, (ii) as a cryogenic liquid, and (iii) as a solid fuel by chemical or physical combination of different materials [1]. Main drawback for storing hydrogen in the form of a pressurized gas is its relatively low energy density. In order to obtain comparable amount of energy with the fossil fuels, pressurized heavy cylinders are required. This is critical in terms of safety and not desired especially in highly populated regions. In storing hydrogen as a cryogenic liquid, the main drawbacks are the high energy requirement for liquefaction and the continuous boil-off of hydrogen. As compared to these two options, storage of hydrogen as a solid fuel offers certain advantages in terms of overall safety and high storage density [1, 3].

Intermetallic compounds (of AB type) can store hydrogen as a solid fuel. Element A is generally a rare earth element or an alkaline earth metal which can form stable hydride(s) and element B, is generally a transition metal that can only form unstable hydrides [2]. Ni is generally used as an element B due to its excellent catalytic properties for hydrogen dissociation [2]. Therefore, properties of stable hydride forming materials can be modified by forming intermetallic compounds; for example, reversibility is increased by the addition of element B.

Recently, Mg-Ni systems have been attracting the attention of materials scientists due to their potential hydrogen storage capacity. Mg_2Ni was found to be low cost, lightweight, low toxic and a reversible hydrogen storage material with high hydrogen storage capacity. It also offers relatively faster absorption/desorption kinetics, especially when used in the nanostructured form [1, 4-14]. Its hydrogen storage capacity is around 3.4 to 3.6 wt.% [1, 4, 5]. Earlier attempts to produce Mg_2Ni involved application of conventional melting. However due to large differences between melting points and vapor pressures of Mg and Ni, this approach was found to be difficult [15]. Some of the other preparatory methods include (i) mechanical alloying [12, 16-18], (ii) vacuum induction melting [19, 20], (iii) vacuum arc melting [21], (iv) combustion synthesis [22], (v) melt-spinning [23], (vi) repetitive rolling [24] and (vii) isothermal evaporation casting [25]. All of these processes require pure metals (Mg and Ni) which again pose the difficulty of protecting the reactive magnesium from oxidation during handling and processing. In order to overcome this difficulty, an alternative approach has been proposed in another study [26]. Electrodeoxidation of MgO-NiO mixtures yielded partial formation of $MgNi_2$ without Mg_2Ni [26]. In the mentioned study, partial formation of $MgNi_2$ was attributed to the incomplete reduction of MgO.

Molten salt electrolysis of $MgCl_2$ is one of the two commonly used industrial processes for the production of elemental magnesium [27]. Therefore, combination of $MgCl_2$ electrolysis and electrodeoxidation of NiO within the same cell to form the desired Mg-Ni intermetallics was investigated in this study. The electrochemical reduction of NiO particles in $MgCl_2$ containing molten salt solutions was followed by electrolysis of $MgCl_2$, which aimed *in-situ* formation of Mg-Ni intermetallics. The experimental conditions were adjusted to favor the formation of the desired Mg_2Ni phase.

2. EXPERIMENTAL

The schematic representation of the experiment setup can be seen in Fig. 1. 0.8 g NiO powder (Sigma Aldrich) was mixed with a binder (PVA, 2% wt.) and die-pressed under 1.5 tons of load. PVA

was evaporated by holding the cylindrical pellets at 600°C for 2 hours. In some of the experiments, the pellets were directly used after this step without sintering, while in some others, they were sintered at 1200°C for 6 hours. Sintered pellets had a diameter of about 1.56 cm and thickness of about 0.12 cm. In some of the experiments employing sintered pellets, ammonium bicarbonate was added to NiO powder to increase the porosity. The percentages of porosities were calculated by Archimedes method before each experiment. Xylene was used as the wetting agent and NiO pellets were held in xylene for 48 hours.

The stoichiometric calculations showed that 2.04 grams of $MgCl_2$ was required to completely convert 0.8 grams of NiO to Mg_2Ni. Four times the stoichiometric amount of $MgCl_2$ was used in the present study. 8.16 grams of anhydrous $MgCl_2$ (Alfa Aesar, Cas: 7786-30-3) was mixed with 46.58 grams of anhydrous $CaCl_2$ (Merck, K36611478 641) and 24.55 grams of NaCl (Sigma Aldrich, Cas: 7647-14-5) to form the electrolyte.

A graphite rod (Alfa Aesar A10134) was used as the anode material. A stainless steel spoon which was welded to a Kanthal wire formed the cathode assembly together with the NiO pellet. The experiments were performed just below the melting point of Mg, 645°C (T_m = 650°C), to avoid possible coalescence of fine magnesium droplets which could hinder the progress of intermetallic formation reaction(s).
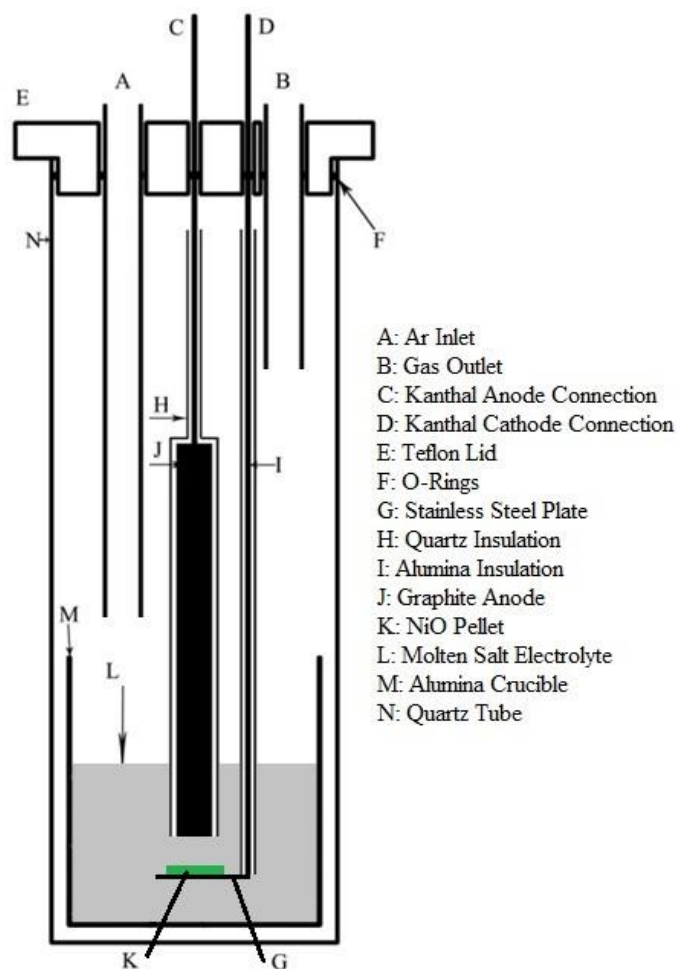

A: Ar Inlet
B: Gas Outlet
C: Kanthal Anode Connection
D: Kanthal Cathode Connection
E: Teflon Lid
F: O-Rings
G: Stainless Steel Plate
H: Quartz Insulation
I: Alumina Insulation
J: Graphite Anode
K: NiO Pellet
L: Molten Salt Electrolyte
M: Alumina Crucible
N: Quartz Tube

Figure 1. Schematic representation of the cell assembly.

The electrodes were immersed into the electrolyte when system was homogenized at 645°C and the experiments were initiated by the application of desired potentials between the electrodes. Table 1 shows the possible reactions which could take place in the present system together with their standard Gibbs energy changes and the corresponding potentials at 645°C:

Table 1. The possible cell reactions with their standard Gibbs Energy changes and the corresponding potentials at 645°C [28-29].

Reaction	ΔG^{o} (J)	E^{o} (V)	No
NiO (s)+ C (s) = Ni + CO (g)	-37100.2	0.19	(1)
$MgCl_2$ = Mg + Cl_2 (g)	491922.4	-2.55	(2)
$MgCl_2$ + 2Ni = $MgNi_2$ + Cl_2 (g)	441108	-2.29	(3)
$MgCl_2$ +(1/2) Ni = (1/2)Mg_2Ni + Cl_2 (g)	469039	-2.43	(4)
$3MgCl_2$ + $MgNi_2$ = $2Mg_2Ni$ + $3Cl_2$	1435048	-2.48	(5)

The potentials required for reactions (2), (3), (4) and (5) further shifts by -150 mV when the activity of $MgCl_2$ in $MgCl_2$ (10.29 wt.%)-$CaCl_2$ (58.75 wt.%)-NaCl (30.96 wt.%) electrolyte is also considered [30]. Fig. 2 shows the variations of reversible cell voltages of the given reactions as a function of temperature.

It can be seen in Fig. 2 that reaction (1) is more favorable than the others. Therefore, NiO can be reduced, without invoking $MgCl_2$ electrolysis, at a potential less than that is required for reaction (3). In addition, following the NiO reduction, the cell potential could be re-adjusted to yield the desired product(s). From the examination of Fig. 2, it can be seen that formations of both $MgNi_2$ and Mg_2Ni, according to reactions (3), (4) and (5), require less potentials than $MgCl_2$ electrolysis, reaction (2).
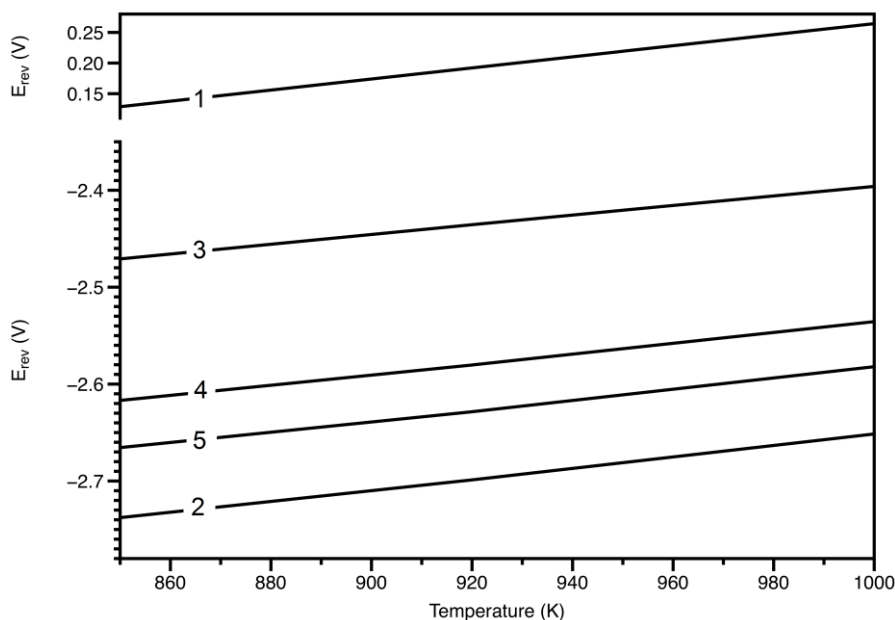

Figure 2. The reversible cell voltage vs. temperature graphs of reactions (1), (2), (3), (4) and (5).

Three different procedures were followed during the application of the cell potential sequences:

1. A three-step procedure included the application of 2.2 V cell potential for 3 hours which was followed by 2.6 V for 16 hours and then 2.7 V for 29 hours.

2. A two-step procedure included the application of 2.4 V cell potential for 3 hours and then 2.7 V for 21 hours.

3. Again a two-step procedure included the application of 2.4 V cell potential for 3 hours and then 2.7 V for 45 hours.

These procedures were selected to successively promote reactions (see Table 1) (1), (3), (5) and/or (4) for procedure 1; and (1), (3), (5) and/or (4) for procedures 2 and 3. The sample preparation information, percent porosities of samples and procedure number indicating the potential sequences for each experiment are given in Table 2. The total durations of test, in hours, are given in the last column of the table inside the parenthesis.

Table 2. The sample preparation information, percent porosity and procedure numbers

Exp. No	Sample Preparation	Percent Porosity	Procedure No (durations, h)
1	Non-sintered	≈43	1 (48)
2	Non-sintered	≈43	2 (24)
3	Sintered	≈40	3 (48)
4	Sintered	≈51	3 (48)

After the experiments, the products were washed with water (30%), ethanol (35%) and methanol (35%) mixture in an ultrasonic mixer. They were collected by filtration, dried in air and then subjected to characterization by x-ray diffraction (Rigaku DMAX 2200 X-Ray Diffractometer). Quantitative analyses of the products were performed by Rigaku software (version 4.2) from X-ray diffractograms. Results of these analyses were verified by mass balance calculations of the raw materials and reaction products.

3. RESULTS AND DISCUSSION

Fig. 3 shows the current-time data recorded during experiments 1, 3 and 4. Sharp increases in applied current at the 3rd and the 18th hours for procedure number 1 correspond to the points where potential was increased from 2.2 to 2.6 V and from 2.6 to 2.7 V, respectively for experiment 1. Similarly the jump in applied current recorded at the 3rd hour for procedure number 3 corresponds to the instance where cell potential was increased from 2.4 to 2.7 V for experiments 3 and 4.
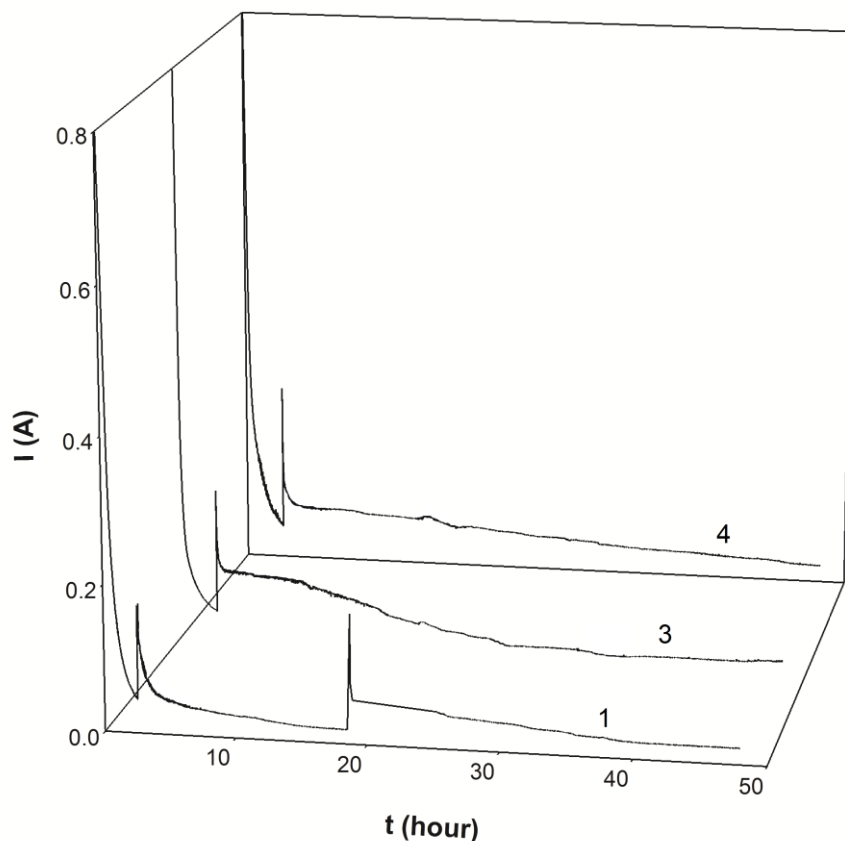
Figure 3. Current-time graph obtained during experiments employing cell potential sequences 1 and 3. Experiment numbers 1, 3 and 4 are given at right for each trace.

Initially applied 2.2 V in experiment 1 allows electrodeoxidation of NiO only, among the reactions given in Table 1. After 3 hours of experiment duration, current levels dropped around 0.05 A which shows that NiO reduction to Ni was almost halted within the first 3 hours. At the 3rd hour, cell potential was increased to 2.6 V which only allows NiO electrodeoxidation and $MgNi_2$ formation according to reaction (3) considering potential losses due to resistances and overpotentials. The current values dropped to very low levels again at around the 18th hour (below 0.02 A). Therefore potential was increased to 2.7 V which only avoids molten salt electrolysis of $MgCl_2$ among the reactions given in Table 1. As it can be seen in Fig. 3, current values again dropped to very low levels (below 0.02 A) at the end of experiment 1 indicating no appreciable progress of the reaction(s).

Similar variations of applied current with time can be seen for experiments 3 and 4 in Fig. 3. After about 26 hours of experiment duration, current values dropped to extremely low values (below 0.009 A) in experiment 3. Although the applied potential of 2.7 V seemed to be high enough for reactions (3), (4) and (5) to proceed, current values dropped to extremely low levels and no appreciable progress of reactions was observed.

When traces of experiments 3 and 4 are examined, it can be seen that after the first three hours, current values dropped to very low values (around 0.05 A). After the potential increase, the current values increased to similar levels in both experiments at first, however, current drop was faster in

experiment 3 than 4. This shows that introduction of pores had a positive effect in the progress of reactions (3), (4) and (5). This observation will be discussed below together with the x-ray diffraction patterns and quantitative analyses results.

The results of quantitative analyses of products obtained by the Rigaku software are given in Table 3. The "*" given in Table 3 indicates the quantities that were below the detection limit. The analyses of experimental data and characterization of products showed partial formation of Mg-Ni intermetallic phases by the present proposed procedure. These results were used to discuss the effects of duration, porosity and sintering on the formations of Mg-Ni intermetallics.

Table 3. Quantitative phase analysis performed by the Rigaku software.

Exp. No	% Ni	% NiO	% MgO	% Mg_2Ni	% $MgNi_2$	% $Mg(OH)_2$
1	43	5	30	11	*	11
2	40	9	37	*	10	4
3	55	18	27	*	*	*
4	18	44	25	*	11	2

3.1. Effect of Duration

Two durations, 24 and 48 hours were used in this study. Figures 4 and 5 show the typical x-ray diffraction patterns of the reduced samples, obtained from experiments 1 and 2 respectively. The peaks for Ni, NiO, MgO, $MgNi_2$, Mg_2Ni and $Mg(OH)_2$ were identified in these figures. It should be noted that some of the small peaks in x-ray diffraction patterns do not belong to Mg and/or Ni containing phases. Several hydrous calcium chloride phases could form in the given experimental conditions. These peaks were left unidentified to prevent confusion. Furthermore, they do not affect the distribution of percentages of Mg and/or Ni containing phases.

The presence of Mg_2Ni was observed in experiment 1 without (or with very little) $MgNi_2$. On the other hand, only $MgNi_2$ was observed in experiment 2. This shows that $MgNi_2$ could be converted to Mg_2Ni in the presence of excess $MgCl_2$, according to reaction (5), when the duration was long. There may also be the possibility of a sluggish kinetics of reaction (5) which can be deduced from the absence of Mg_2Ni in experiment 2.
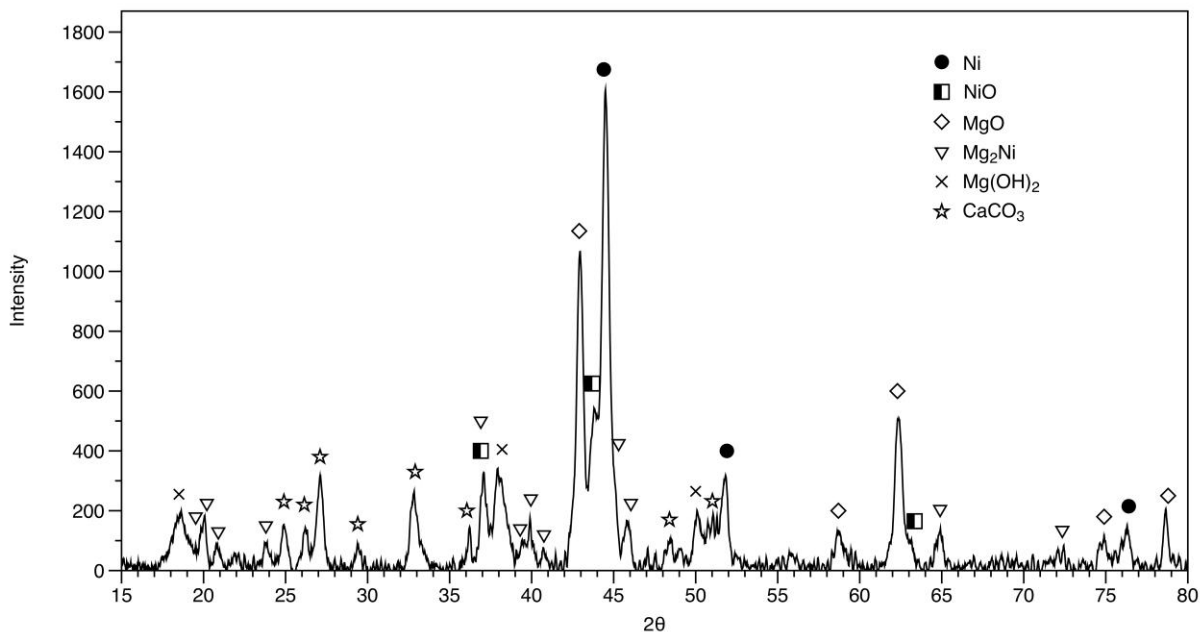
Figure 4. X-ray diffraction result of the sample obtained after experiment 1.
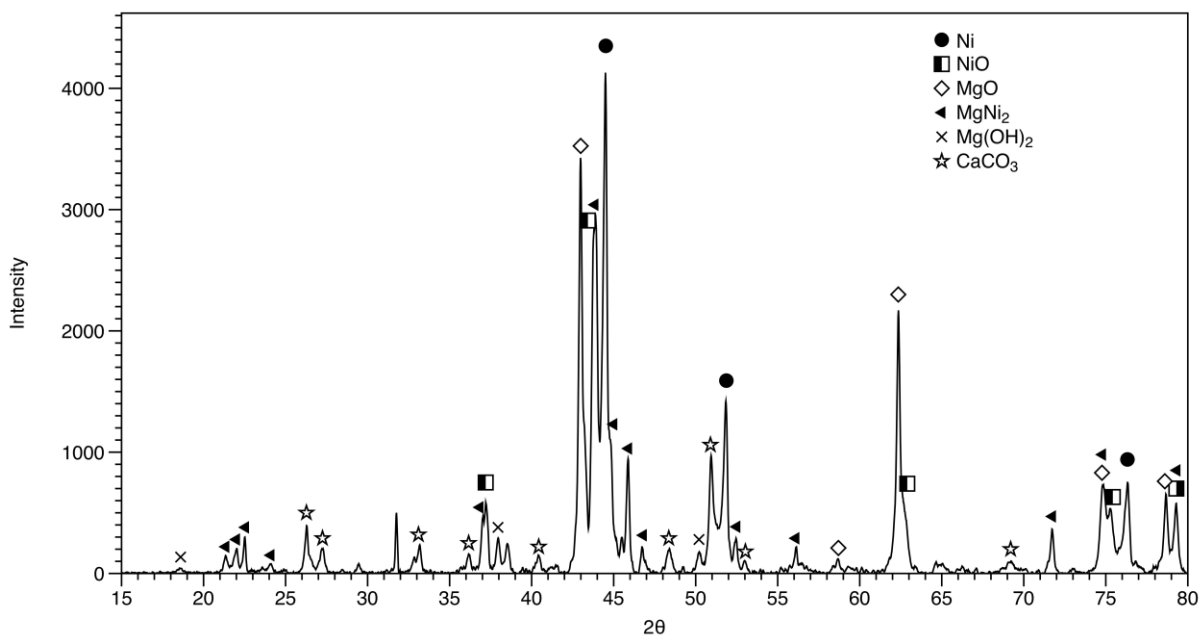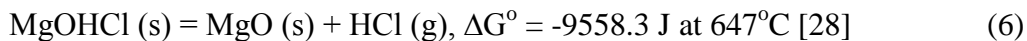

Figure 5. X-ray diffraction result of the sample obtained after experiment 2.

The presence of MgO in the reduced samples was considered to be mainly due to the hygroscopic nature of $MgCl_2$. Any moisture left in the cell feed could lead to formation of MgOHCl [31] upon heating. Further heating causes this compound to spontaneously decompose to MgO and HCl [28] according to reaction (6). Once it is formed, MgO is expected to move to the cathode and stay there, when the electrophoresis effect and the density of MgO are considered [32, 33].

MgOHCl (s) = MgO (s) + HCl (g), ΔG^o = -9558.3 J at 647°C [28]   (6)

The presence of $Mg(OH)_2$ was explained with reference to the spontaneous reactions of Mg-Ni intermetallics with water [28, 29]. The extent of spontaneous reaction was reported to take place slowly to convert all Mg-Ni intermetallics to $Mg(OH)_2$ in 120 hours during washing treatment in water [34]. Besides, it was found that $Mg(OH)_2$ is more stable than MgO at room temperature, therefore $Mg(OH)_2$ was expected to remain as it is once formed [28]. Considering the amounts of Mg-Ni intermetallics and $Mg(OH)_2$ calculated by quantitative analysis of Rigaku software, it can be seen that relatively longer experimental durations favor the formation of Mg_2Ni phase.

The reduced sample was weighted approximately 1.4 grams following the drying in experiment 1. Stoichiometric calculations showed that initial Ni amount was 0.63 grams. However, the total Ni amount in the reduced sample after experiment 1 was calculated as 0.57 grams from quantitative analysis of Rigaku (version 4.2) considering all of the peaks of the diffraction. This adds to the reliability of quantitative analysis software (Rigaku (version 4.2)). In spite of many interactions between the pellet, the cathode connection and/or other parts of experimental setup, and losses that may occur during collection from the cathode and/or during washing, over 90% of Ni appears in the quantitative analysis.

3.2. Effect of Sintering and Porosity

Results of experiments 1, 3 and 4 given in Table 3 can be used to determine the effects of sintering and porosity on the formation of Mg-Ni intermetallics. Figures 6 and 7 show the x-ray diffraction patterns of samples, obtained after experiments 3 and 4 respectively.
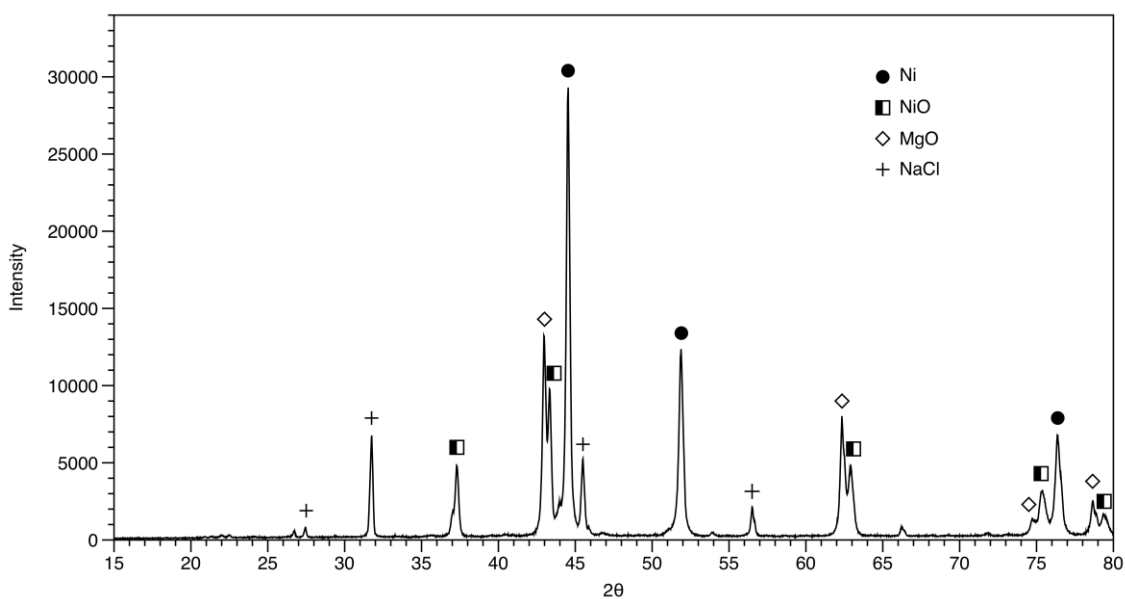

Figure 6. X-ray diffraction pattern of the sample obtained after experiment 3.
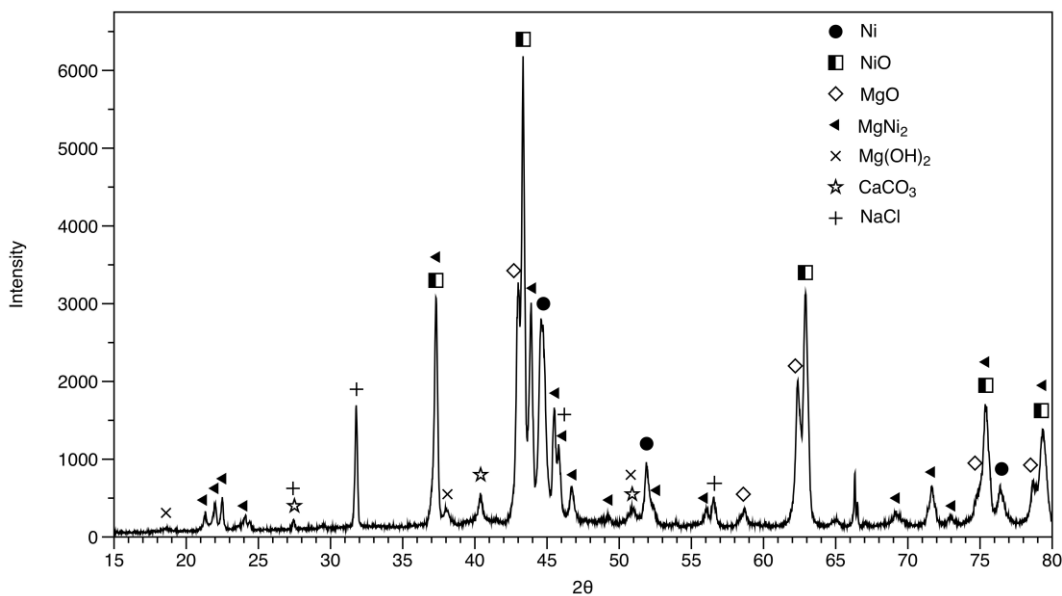
Figure 7. X-ray diffraction pattern of the sample obtained after experiment 4.

Calculations suggested that at least 64.2 % open porosity was required to compensate the large difference between the molar volumes of Mg-Ni intermetallics and NiO when all the NiO is converted to Mg_2Ni. Insufficient porosity of NiO, in experiment 3, could be the reason for the absence of any Mg-Ni intermetallic phase. Unlike experiment 3, 11% $MgNi_2$ was formed in 4 in which ammonium bicarbonate (about 8%) was mixed to the NiO pellet to increase its porosity. However, as can be seen in Table 3, increased porosity resulted in higher amounts of unreduced NiO. Therefore, when the results of experiments 3 and 4 are compared, it can be concluded that increase in porosity increased Mg-Ni intermetallic formation; nevertheless, it slowed down NiO electrodeoxidation because pores were expected to slow down charge transfer [35, 36].

Unlike the sintered pellets, products of the non-sintered NiO pellets were found to be dispersed, at the cathode. One of the possible reasons for higher Mg-Ni intermetallic formation in experiment 1, could be the creation of space by the dispersed nickel, resulting in higher surface area for intermetallic phase formation. During electrodeoxidation of NiO to Ni, shrinkage is expected which results in decreased porosity as compared to its initial value. Moreover, as the atomic radius of Mg is larger than that of Ni, even with higher porosities, it is difficult to produce Mg_2Ni, when Mg starts diffusing to the inner lattice of the Ni particles. Besides, crystal structures of Mg and Mg_2Ni are hexagonal close packed (HCP) and that of Ni is face centered cubic (FCC). Both diffusion, being a kinetically slower process, and the requirement for the formation of a HCP crystal structure may impose limitations on the extent of formation of Mg_2Ni phase.

It is important to note that although experimental durations were very long, NiO peaks were present in all the reduced samples (Figures 4, 5, 6 and 7). However, the electrochemical reduction of NiO in the absence of $MgCl_2$ was reported to be completed in a similar setup at $800^{\circ}C$ [26]. In the present study, the presence of $MgCl_2$ in the electrolyte, limited the operating temperature and applied potential during NiO reduction to avoid the electrolysis of $MgCl_2$. Another point is that the formation

of lower conducting MgO, throughout the experiments, might have slowed down the passage of electrical charge.

The progress of an electrochemical process can easily be followed from the accumulative electrical charge versus time graph because the amount of material reduced is proportional to the accumulative charge that passes through the cell according to Faraday`s law. Therefore experiments can easily be compared with each other, when similar current efficiencies are assumed. The equations for determining the amount of material reduced, W, and the accumulated charge, Q, during an experiment are as follows:

$$W = \frac{MItX}{100nF} \qquad (7)$$

$$Q = \int_{t=0}^{t=tf} I dt \qquad (8)$$

where M is the molecular weight of the reduced material, I is current in A, t is time in seconds, X is percent current efficiency, n is the number of Faradays involved and F is the Faraday constant (96 500 Coulomb/gram-equivalent).

Calculations showed that at least 2067 C of accumulated charge was required to pass through the cell to fully reduce 0.8 g NiO to Ni. Additional (at least) 6784 C of accumulated charge was required for complete reaction of Ni with $MgCl_2$ to yield Mg_2Ni. Fig. 8 shows the total charge passed versus time graphs of experiments 3 and 4.
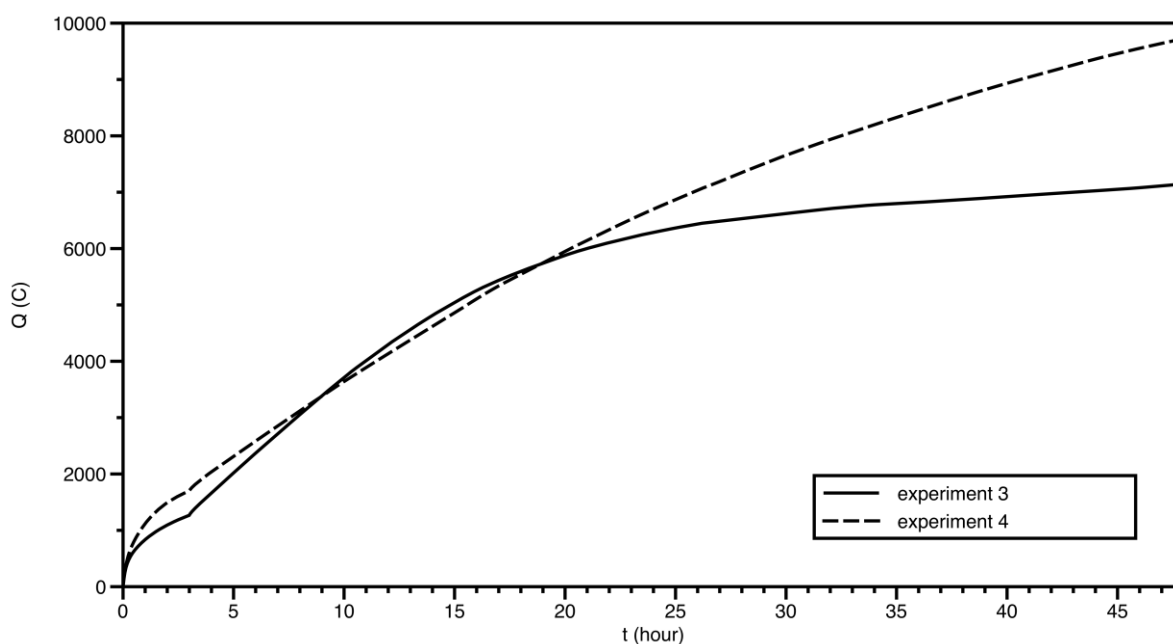
Figure 8. Total Charge passed versus time graphs of experiments 3 and 4.

From Fig. 8, it can be seen that the total charge passed during experiment 4 at the end of 48 hours was higher than experiment 3. In fact, the obvious difference between experiment 3 and 4 began

after about 19th hour, when reactions (3), (4) and (5) were expected to proceed in both cases. The slightly higher accumulated charge passed in the initial period and lower NiO concentration of the product for experiment 3 suggests faster NiO electrodeoxidation for this case, but it is clear that progress of electrochemical reaction of experiment 3 slows down after the initial period. This may be accounted to lower porosity of NiO pellet that could not provide the additional volume during intermetallic formation.

Combination of $MgCl_2$ electrolysis and electrodeoxidation of NiO within the same cell to form the desired Mg-Ni intermetallics was investigated in this paper. The electrochemical reduction of NiO particles in $MgCl_2$ containing molten salt solutions was followed by electrolysis of $MgCl_2$, which aimed *in-situ* formation of Mg-Ni intermetallics. The authors believe that the difficulties arise during handling, preparation and processing due to highly reactive nature of magnesium can be eliminated by such a process. However, the process is not limited to Mg-Ni intermetallics and can be expanded to include intermetallic compounds that can be produced by the combination of electrodeoxidation and molten salt electrolysis techniques.

4. CONCLUSIONS

Partial formations of Mg_2Ni and $MgNi_2$ intermetallics were achieved by combining electrochemical reduction of NiO and molten salt electrolysis of $MgCl_2$.

Incomplete reduction of NiO was attributed to the limitations in operating temperature and applied potential due to the presence of $MgCl_2$ in the electrolyte.

Sintering of NiO pellets affected Mg-Ni intermetallic formation negatively. In addition, experiments with sintered pellets showed that increase in porosity had a positive effect on Mg-Ni intermetallic formation. This is in keeping with the expectations because both Mg_2Ni and $MgNi_2$ have larger molar volumes when compared to NiO.

Increase in experiment duration had a positive effect on the formation of Mg_2Ni. $MgNi_2$ was found to be converted to Mg_2Ni in the presence of excess $MgCl_2$, especially at longer electrolysis durations. Alternative procedures could be tested to enhance the formation of Mg_2Ni.

References

1. B. Sakintuna, F. Lamari-Darkrim, M. Hirscher, *Int. J. Hydrogen Energ.*, 32 (2007) 1121-1140.
2. Züttel, A, Mater. Today, 6 (2003) 24-33.
3. R.C. Weast, M.J. Astle, W.H. Beyer, CRC Handbook of Chemistry and Physics 64th ed., Boca Raton, FL, CRC Press, 1983.

4. R. Vijay, R. Sundaresan, M.P. Maiya, S. Srinivasa Murthy, *Int. J. Hydrogen Energ*., 30 (2005) 501-508.
5. M. Abdellaoui, D. Cracco, A. Percheron-Guegan, *J. Alloys Compd*., 268 (1998) 233-240.
6. J.L. Iturbe Garcia, B.E. Lopez-Munoz, R. Basurto, S. Millan, *Rev. Mexç Fis*., 52 (2006) 365-367.
7. U. Haussermann, H. Blomqvist, D. Noreus, *Inorg. Chem*., 41 (2002) 3684-3692.
8. S.S. Han, N.H. Goo, K.S. Lee, *J. Alloys Compd*., 360 (2003) 243-249.
9. S. Orimo, H. Fujii, *Appl. Phys*. A, 72 (2001) 167-186.
10. T. Sato, H. Blomqvist, D. Noreus, *J. Alloys Compd*., 356-357 (2003) 494-496.
11. M. Zhu, H. Wang, L.Z. Ouyang, M.Q. Zeng, *Int. J. Hydrogen Energ*., 31 (2006) 251-256.
12. A. Zaluska, L. Zaluski, J.O. Ström-Olsen, *J. Alloys Compd*., 289 (1999) 197-206.
13. M. Abdellaoui, S. Mokbli, F. Cuevas, M. Latroche, A.P. Guegan, H. Zarrouk, *J. Hydrogen Energ*., 31 (2006) 247-250.
14. L. Zaluski, A. Zaluska, P. Tessier, J.O. Ström-Olsen, R. Schulz: *J. Alloys Compd*., 217 (1995) 295-300.
15. Y. Jin, X. Yang, Y. Li, W. Zhang, *Mod. Appl. Sci*., 4 (2010) 114-118.
16. G. Liang, S. Boily, J. Hout, A. Van Neste, R. Schulz, *J. Alloys Compd*., 267 (1998) 302-306.
17. M.Y. Song, *Int. J. Hydrogen Energ*., 20 (1995) 221-227.
18. L. Aymard, M. Ichitsubo, K. Uchida, E. Sekreta, F. Ikazaki, *J. Alloys Compd*., 259 (1997) L5-L8.
19. N. Terashita, M. Takahashi, K. Kobayashi, T. Sasai, E. Akiba: *J. Alloys Compd*., 293-295 (1999) 541-545.
20. T. Spassov, U. Köster: *J. Alloys Compd*., 287 (1999) 243-250.
21. H. Shao, T. Liu, X. Li, L. Zhang, *Scr. Mater.,* 49 (2003) 595-599.
22. L. Li, T. Akiyama, J-i.Yagi, *J. Alloys Compd*., 308 (2000) 98-103.
23. G. Friedlmeier, M. Arakawa, T. Hirai, E. Akiba, *J. Alloys Compd*., 292 (1999) 107-113.
24. T.T. Ueda, M. Tsukahara, Y. Kamiya, S. Kikuchi, *J. Alloys Compd*., 386 (2005) 253-257.
25. C. Hsu, S. Lee, R. Jeng and J. Lin, *Int. J. Hydrogen Energ*., 32 (2007) 4907-4911.
26. S. Tan, K. Aydınol, T. Öztürk, İ. Karakaya, *J. Alloys Compd*., 504 (2010) 134-140.
27. G. Demirci, İ. Karakaya, *J. Alloys Compd*., 439 (2007) 237-242.
28. Facility for the Analysis of Chemical Thermodynamics, 2012, Retrieved from http://www.crct.polymtl.ca/fact/
29. J.F. Smith, J.L. Christian, *Acta Metall*., 8 (1960) 249-255.
30. İ. Karakaya, W.T. Thompson, *Can. Metall*. Q. 25 (1986) 307-317.
31. İ. Karakaya, "Electrochemical Determination of Thermodynamic Properties of Magnesium Cell Electrolyte the system $MgCl_2$-NaCl-$CaCl_2$", Ph. D. Thesis submitted to McGill University, 1985.
32. Chemical Book.com, 2013, Retrieved from: http://www.chemicalbook.com/ProductChemicalPropertiesCB8853024_EN.htm
33. O. O. Van der Biest, L. J. Vandeperre, *Annu. Rev. Mater. Res*., 29 (1999) 327-352.
34. H. Wang, L. Han, H. Hu, D.O. Northwood, *J. Alloys Compd*., 470 (2009) 539-543.
35. R. L. Centeno-Sanchez, D. J. Fray, G. Z. Chen, *J. Mater. Sci*., 42 (2007) 7494-7501.
36. E. Ergül, İ. Karakaya, M. Erdoğan, F. Erden, in: EPD Congress 2012, TMS, 2012.